Magnetic and structural properties of the double-perovskite Ca_2FeReO_6

W Westerburg†, O Lang‡, C Felser‡, W Tremel‡, M Waldeck§, F Renz§, P Gütlich§, C Ritter‖ and G Jakob†*

†*Institut für Physik, Johannes Gutenberg-Universität Mainz, Staudinger Weg 7, 55099 Mainz, Germany*

‡*Institut für Anorganische Chemie und Analytische Chemie, Johannes Gutenberg-Universität Mainz, Duesbergweg 10-14, 55099 Mainz, Germany*

§*Institut für Anorganische Chemie und Analytische Chemie, Johannes Gutenberg-Universität Mainz, Staudinger Weg 9 , 55099 Mainz, Germany*

‖*Institute Laue Langevin, 6, rue Jules Horowitz, Boîte Postale 156, 38042 Grenoble-Cedex 9, France*

(17 April 2000)

We suceeded in the preparation of polycrystalline Ca_2FeReO_6 which has a Curie temperature T_C of 540 K, the highest value of all magnetic perovskites investigated up to now. This material has been characterised by X-ray and neutron powder diffraction. We found at 548 K a monoclinic unit cell (space group $P2_1/n$) with $a = 5.4366(5)$ Å, $b = 5.5393(5)$ Å, $c = 7.7344(5)$ Å, and $\beta = 90.044(4)^\circ$. For low temperatures a phase separation in two monoclinic phases with identical cell volume is observed in neutron scattering. The two phases possess different magnetic structure and coercivity. ^{57}Fe-Mössbauer spectroscopy measurements show the presence of four different Fe^{3+} positions indicating two different phases at room temperature, indistinguishable in the diffraction experiments. The conductivity is thermally activated for all temperatures and no significant magnetoresistivity is observed.

PACS numbers: 61.12.-q, 76.80.+y, 75.50.Gg, 75.25.+z, 61.10.Nz

I. INTRODUCTION

The advent of spin based electronics has lead to a strong interest in materials with high spin polarisation. Among these half-metallic oxides are promising candidates for future applications as magnetoresistive devices. At low temperatures impressive performance of spin polarised tunneling devices has been reported[1]. However, the increase of spin fluctuations with increasing temperature is a severe obstacle for room temperature applications of materials with low Curie temperatures. Therefore both high spin polarisation and high Curie temperatures are important requirements. Recently, a large room temperature magnetoresistance was found in Sr_2FeMoO_6[2], a material belonging to the class of double-perovskites ($AA'BB'O_6$)[3] with a Curie temperature above 400 K. In this report we present a detailed study of Ca_2FeReO_6 (CFRO), the double-perovskite with the highest Curie temperature ($T_C = 540$ K).

II. EXPERIMENT

The compound Ca_2FeReO_6 was synthesised by a solid-state reaction from CaO (Alfa, 99.95%), ReO_3 (Alfa, 99.9%), Fe (Alfa, 99.998%) and Fe_2O_3 (Alfa, 99.99%) using the stoichiometric ratio of 2:1:$\frac{1}{3}$:$\frac{1}{3}$ respectively and batches of an overall mass of 2 g. The well grained sample was transferred into a corundum container and sealed in an evacuated quartz tube ($p = 5 \times 10^{-5}$ mbar). The tube was heated to 1173 K with a rate of 1 K/min and held at this temperature for 48 hours. After cooling the sample to room temperature with a rate of 5 K/min the sample was reground and resealed. The resealed sample was annealed at 1173 K for 14 days and then quenched with liquid nitrogen. This method yielded a black polycrystalline product.

X-ray diffraction was performed at room temperature using a Philips X'Pert MPD diffractometer in Bragg-Brentano geometry. The instrument works with Cu K_α radiation ($\lambda = 1.5418$ Å).

At the Institut Laue Langevin in Grenoble the neutron powder diffraction data were collected on the high-resolution instrument D2B with the sample (10 g) placed in a cylindrical vanadium can inside a cryofurnace. A wavelength of $\lambda = 1.594$ Å over an angular range of 0° and 162° was used. We measured on warming at several fixed temperatures of 2, 100, 200, 300, 400, 444, 524 and 548 K. The structural and magnetic parameters gained with X-ray and neutron diffraction were refined by the Rietveld method using the program FULLPROF[4]. For the line shape a pseudo-Voigt function was selected. All Bragg peaks could be identified and therefore no regions were excluded in the refinement.

The magnetic properties as AC magnetic susceptibility and DC magnetic moment were determined with a Lake Shore 7000 magnetometer and a SHE SQUID magnetometer, respectively.

The temperature dependence of the resistivity was measured by the standard four-point technique in a standard cryostat with a 12 T superconducting magnet.

III. CRYSTAL STRUCTURE

A. Neutron Diffraction

Over 300 compounds are known in the class of double-perovskites ($AA'BB'O_6$). The B, B'-ions arrange in three different manners, rock-salt, random and in rare cases layered. Which type of configuration exists, depends on the charge, size, electronic configuration, and A/B size ratio of the involved ions. In the case of CFRO the charge difference is $2e$ (Fe^{3+}, Re^{5+}, see Mössbauer measurements below) and the ionic radius difference is 0.065 Å. The unit cell for rock-salt arrangement can be derived either from a cubic $2a_0$ or a monoclinic ($\sqrt{2}a_0 \times \sqrt{2}a_0 \times 2a_0$) cell, where a_0 is the lattice parameter for the standard cubic perovskite ABO_3 ($a_0 \approx 4$ Å). The monoclinic cell is favoured if the tolerance factor t defined in Eq. 1 is less than unity.

$$t = \frac{\frac{r_A + r_{A'}}{2} + r_O}{\sqrt{2}\left(\frac{r_B + r_{B'}}{2} + r_O\right)} \qquad (1)$$

The cation order is revealed in the cubic case by the presence of (hkl) reflections with $h, k, l = 2n + 1$ or in the monoclinic case by $(0kl)$ reflections with $k = 2n + 1$, respectively. For CFRO due to the low tolerance factor of $t = 0.89$ a monoclinic unit cell is expected (ionic radii from Ref.[5]). A similar compound Ca_2FeMoO_6 also a ferrimagnetic oxide with $t = 0.88$ was found recently to have a monoclinic unit cell[6].

The diffraction pattern recorded at D2B above T_C at $T = 548$ K is shown in Fig. 1. A slight impurity phase of 0.5% of Fe_3O_4 (due to reaction $3Fe_2O_3 \rightarrow 2Fe_3O_4 + \frac{1}{2}O_2$) could be detected for all temperatures. The pattern was refined in the space group $P2_1/n$. The positional and thermal paramaters are listed in Table I. The monoclinic unit cell results from rotations of the BO_6, $B'O_6$ octahedra. Fe and Re are indistinguishable for neutrons in the paramagnetic regime due to the small difference in the nuclear coherent scattering lengths of 9.45 fm and 9.20 fm, respectively. However, in the ferromagnetic regime they can be discerned due to interaction of the neutron with the magnetic moment of the electron shells. Additionally, the structure was checked with X-ray diffraction (see below). The refinements show that the Fe atoms occupy the $2d$ position $(\frac{1}{2}, 0, 0; 0, \frac{1}{2}, \frac{1}{2})$ and Re the $2c$ position $(0, \frac{1}{2}, 0; \frac{1}{2}, 0, \frac{1}{2})$, i.e. there exists an ordered rock-salt arrangement. The A atom and three oxygen atoms occupy different $4e$ positions. The monoclinic unit cell with tilts of the octahedra is shown in Fig. 2. According to Glazer's notation we have $a^-a^-b^+$ along the pseudocubic axes[7]. The superscripts indicate that neighbouring octahedra along the corresponding axis rotate in the same (+) or opposite (-) direction. The view in Fig. 2a is along the pseudocubic a (or b) axis (view along the crystallographic (110) direction) and shows octahedra rotations with opposite sign. Part b of the figure shows the view along the crystallographic c axis showing the in phase rotation of the octahedra along this axis.

With decreasing temperature we observed an unusual peak broadening and finally a peak splitting of selective nuclear Bragg reflections with a large momentum transfer along the unique b axis. Such an unusual broadening of peaks, which have a large component along the unique axis, was also observed in perovskite manganites $Nd_{1-x}Sr_xMnO_3$ which belong to the same space group[8]. Although the best refinement was achieved in this case using two distinct phases the origin of the peak broadening has been attributed to the existence of strain effects. The clear splitting of the (040) reflection visible in the diffraction pattern as shown in Fig. 3, however, cannot originate from strain effects and clearly two distinct phases are required. In our refinement we used two crystallographic phases and two magnetic phases of CFRO and a impurity phase of 0.5% of magnetite, together five phases. The pattern taken at 2 K is shown in Fig. 4. The two phases of CFRO differ mostly in the values of the b axes and the β angles but have almost the same unit cell volume. In Table II the positional and thermal paramaters of the two phases are shown. The results for the lattice constants and the β angles of all refinements are listed in Table III and presented in Fig. 5. From 2 K up to 300 K the two phases have almost the same weight in the refinement but the difference in lattice parameters between the two phases decreases with increasing temperature. At temperatures of 400 K and higher the $(0k0)$ reflections are symmetric, which is depicted in Fig. 3, and neutron refinement shows a single phase. It is unresolved if the two phases are just similar and can no longer be crystallographically distinguished or whether a true phase separation of a single high temperature phase takes place below 400 K. The bond length and bond angles are presented in Table IV showing again the distorted perovskite structure.

B. X-ray Diffraction

The X-ray powder diffraction pattern of CFRO were taken at room temperature. The data are shown in Fig. 6. No impurity phase could be detected. Due to the strongly distorted perovskite structure the pattern shows a large amount of Bragg peaks. The results of the structure refinement are in agreement with the data gained by neutron diffraction. Due to the high absorption of X-rays in the Re-compound, however, the X-ray refinement has larger errors. Nevertheless, the high intensity of the (011) and $(\overline{1}01)$, (101) reflections indicate the rock-salt arrangement of the Fe, Re sublattice and the refinement yields a high degree of order (less than 2% interchanged Fe, Re atoms). Due to the lower intensity only one phase was refined. The refined cell parameters of $a = 5.417(2)$ Å, $b = 5.543(2)$ Å, $c = 7.706(2)$ Å, and $\beta = 90.03(3)^\circ$ are shown in Fig. 5 by crosses.

IV. MAGNETIC PROPERTIES

For CFRO a Curie temperature of 540 K is reported in literature[9]. However, a detailed investigation of the magnetic properties is still missing. Therefore we measured AC susceptibility, overall and local magnetic moment and magnetic hysteresis.

A. Magnetic susceptibility

In Fig. 7 we show the temperature dependence of the AC susceptibility. Besides the ferro(i)magnetic transition at 540 K, which is visible in the inset, there are two further anomalies in the AC susceptibility. There is a slight temperature dependence of χ' from room temperature down to 125 K. At this temperature the susceptibility becomes temperature independent and there is a small anomaly also in the loss component χ''. A clear magnetic phase transition exists at 50 K showing up as a sharp decrease of χ' and a sharp maximum in χ''. These anomalies are frequency independent (the measurement taken at 7 Hz not presented in Fig. 7 shows the same anomalies) but they do not show up in the temperature dependence of the DC magnetic moment.

B. DC magnetisation

Measurements of the DC magnetisation show ferromagnetic hysteresis loops. A full saturation of the magnetic moment at low temperatures is not achieved in fields of $\mu_0 H = 1$ T. The unusual shape of the low temperature hysteresis curves can be understood by a superposition of two magnetic phases with high and low coercivity, respectively. They contribute approximately equal to the total magnetic moment as is sketched in Fig. 8. We attribute these two phases to the two different crystallographic phases which possess different anisotropy energies. With increasing temperature the magnetic phase of high coercitivity becomes 'softer' and the hysteresis curves of both phases merge to a nearly normal ferromagnetic hysteresis loop. The remnant magnetic moment of 1.3 $\mu_\mathbf{B}$/f.u. is temperature independent below 250 K while the total coercivity increases from 11 mT at 250 K to 0.13 T at 4 K.

C. Magnetic structure from Neutron Scattering

Due to the different number of d-electrons in the shells Fe and Re are distinguishable magnetically for neutrons in the ferromagnetic regime. Large magnetic contributions to the (011) and (101) Bragg peaks are visible around 20.5° at low temperatures. The nuclear contribution to these peaks is negligibly small. To the best of our knowledge the neutron scattering form factor of Re^{5+} is unknown and we approximated it using the values for Mo^{3+}[10]. Within this approximation the best refinements were obtained with a ferrimagnetic arrangement of the Fe and Re spins for one phase and a ferromagnetic alignment of the Fe spins for the other phase. The magnetic moments at the Fe and Re positions are 4.0(2) and -0.81(6), respectively for phase 1 and 4.2(2) and -0.1(6), respectively for phase 2. In both phases best refinements were achieved for spin orientations along the [110] direction. We obtained at 2 K a Bragg factor of 4.7% and 4.2% for the two phases. The temperature dependence of the (011) and (101) Bragg peaks is shown in Fig. 9. The magnetic contribution decreases with increasing temperature and vanishes at T_C. The magnitude of the refined magnetic moment disagrees with the DC magnetisation result. In a magnetic field of $\mu_0 H = 1$ T one should reach in DC magnetisation a value close to saturation, while we only observe $\approx 1.5\mu_\mathbf{B}$/f.u.. We do not expect the approximative use of the form factor to be responsible for the discrepancy and since the temperature dependence of the low angle peaks confirms their magnetic origin, we consider the neutron result more reliable. Further investigations such as solving the spin-structure of CFRO are necessary to elucidate this problem.

V. ^{57}FE-MÖSSBAUER MEASUREMENTS

To gain further information of the valence and the electronic state of the iron in the compound ^{57}Fe-Mössbauer measurements were performed. Natural iron was used for preparation of the sample which contains only 2.2% ^{57}Fe. The presence of Re in the sample caused some difficulties because of its strong absorption for γ-rays. The L-I, L-II, and L-III absorption edges of Re have an energy slightly below the 14.4 keV γ-quanta, which are used for ^{57}Fe-Mössbauer measurements. Therefore the resulting spectra have a low relative transmission and are difficult to fit.

Mössbauer spectra of CFRO were recorded at 4.2 K and 293 K in two different apparatures. Each spectrum has been taken for one week. Mössbauer transmission spectra were taken with a constant acceleration spectrometer, using a 1024 channel analyser in the time mode. For the 4.2 K measurement a Na(Tl)I scintillator was used while the 293 K measurement was done with a proportional counter. A 50 mCi ^{57}Co source in a rhodium matrix at ambient temperature was used in both cases. The spectra were fitted with the Mössbauer analysis program *effi*[11].

^{57}Fe-Mössbauer spectra were used to resolve the valence and electronic state of the iron in the compound. The Mössbauer data are shown in Fig. 10 and Table V. For both temperatures a six-line pattern, which is typical for magnetically long range ordered systems[12], was obtained. At 293 K, Mössbauer spectroscopy revealed four iron sites which is understood, knowing the presence of

two phases from neutron diffraction measurements with two different Fe sites for each phase. Both spectra were fitted with natural line width. In each phase, the isomer shift δ and the quadrupole splitting $\Delta E_{\rm Q}$ were taken correlated, while the magnetic splitting $B_{\rm hf}$ appeared to be different for all four sites. At 4.2 K, the difference in the magnetic splittings diminished so that two sites in each phase appear almost indistinguishable. Such a behaviour is typical for magnetic systems approaching magnetic saturation.

The subspectrum with an isomer shift $\delta = 0.004(5)$ mm/s at ambient temperature and $\delta = 0.139(6)$ mm/s at 4.2 K results from an Fe^{3+}-impurity in the Be-window of the proportional counter.

The hyperfine fields are in the same range as those for the analogous Ba compound Ba_2FeReO_6 measured by Sleight and Weiher[13]. In the recent study on Ca_2FeMoO_6 the values for the magnetic fields are almost the same[14]. There they found at 4.2 K two iron sites in the ratio 0.44 : 0.56. Unfortunately no satisfying conclusion can be drawn on whether the irons are in two phases with one site or in one phase with two sites.

In CFRO the value for quadrupole splittings is practically temperature independent, which is typical for Fe^{3+} high spin in octahedral site[15]. Also the shifts, quadrupole splittings, and hyperfine fields are in the range of a typical Fe^{3+} in the high-spin state in nearly octahedral environment[12].

VI. TRANSPORT PROPERTIES

In Fig. 11 the longitudinal resistivity of CFRO is shown. The room temperature value of 17 mΩcm is comparable with other reported results[16]. The temperature dependence shows a thermally activated behaviour. Down to 4 K the resistivity increases more than three orders of magnitude to 53 Ωcm at 2.7 K. Even in magnetic fields of $\mu_0 H = 8$ T no magnetoresistance was observed over the whole temperature range. This is in contrast to the similar compound Ca_2FeMoO_6 which shows a metallic behaviour and a large magnetoresistance[6]. Closer inspection of data reveals a change in conduction mechanism. Below 20 K the resistivity increases strictly logarithmic with decreasing temperature, as shown in the inset of Fig. 11. Above 110 K the temperature dependence of the resistivity is variable range hopping like, $\rho \propto \exp((T_0/T)^{0.25})$. A similar behaviour of the resistivity was found in disordered Sr_2FeMoO_6 thin films[17].

VII. CONCLUSIONS

In summary, we have investigated the crystal structure, the transport and magnetic properties of polycrystalline double-perovskite Ca_2FeReO_6. We found a monoclinic unit cell with rock-salt order of the Fe and Re ions. Below $T_C = 540$ K the material is magnetically ordered. By Mössbauer measurements a typical Fe^{3+} state was revealed. For low temperatures a phase separation in two monoclinic phases with identical cell volume is observed in neutron scattering. The two phases possess different magnetic structure and coercivity. The temperature dependence of the resistivity exhibits a thermally activated behaviour and shows no magnetoresistance over the whole temperature range. Diffraction measurements on a single crystal are necessary to identify the origin of the phase separation.

ACKNOWLEDGMENTS

This work was supported by the Deutsche Forschungsgemeinschaft through Project JA821/1-3, Gu95/47-2 and the Materialwissenschaftlichen Forschungszentrum (MWFZ) Mainz. The ILL laboratory is acknowledged for granting beam time. We thank J. Ensling, H. Spiering, and H.J. Elmers for useful discussions about Mössbauer and magnetisation measurements.

---

* Electronic address: jakob@mail.uni-mainz.de

[1] Gupta A and Sun J Z 1999 *J. Magn. Magn. Mater.* **200** 24
[2] Kobayashi K I, Kimura T, Sawada H, Terakura K and Tokura Y 1998 *Nature* **395** 677
[3] Anderson M T, Greenwood K B,Taylor G A and Poeppelmeier K R 1993 *Prog. Solid. St. Chem.* **22** 197
[4] Rodríguez-Carvajal J 1993 *Physica* B **192** 55
[5] Shannon R D 1976 *Acta Crystallogr.* A **32** 751
[6] Alonso J A, Casais M T, Martínez-Lope M J, Martínez J L, Velasco P, Muñoz A and Fernández-Díaz M T 2000 *Chem. Mater.* **12** 161
[7] Glazer A M 1972 *Acta Crystallogr.* B **28** 3384
[8] Kajimoto R, Yoshizawa Y, Kawano H, Tokura Y, Ohoyama K and Ohashi M 1999 *Phys. Rev.* B **60** 9506
[9] Longo J and Ward R 1961 *J. Amer. Chem. Soc.* **83** 2816
[10] Wilkinson M K, Wollan E O, Child H R and Cable J W 1961 *Phys. Rev.* **121** 74
[11] Gerdau E and de Waard H 2000 *Hyperfine Interact.* **125** 197
[12] Greenwood N N and Gibb T C 1977 *Mössbauer Spectroscopy* (London: Chapman and Hall Ltd)
[13] Sleight A W and Weiher J F 1972 *J. Phys. Chem. Solids* **33** 679
[14] Pinsard-Gaudart L, Suryanarayanan R, Revcolevschi A, Rodríguez-Carvajal J, Greneche J M, Smith P A I, Thomas R M, Borges R P and Coey J M D 2000 *MMM Proc.* at press
[15] Gütlich P, Link R and Trautwein A 1978 *Mössbauer Spectroscopy and Transition Metal Chemistry* (Berlin: Springer)

[16] Prellier W, Smolyaninova V, Biswas A, Galley C, Greene R L, Ramesha K and Gopalakrishnan J 2000 *J. Phys. Condens. Matter* **12** 965
[17] Westerburg W, Martin F and Jakob G 2000 *MMM Proc.* at press

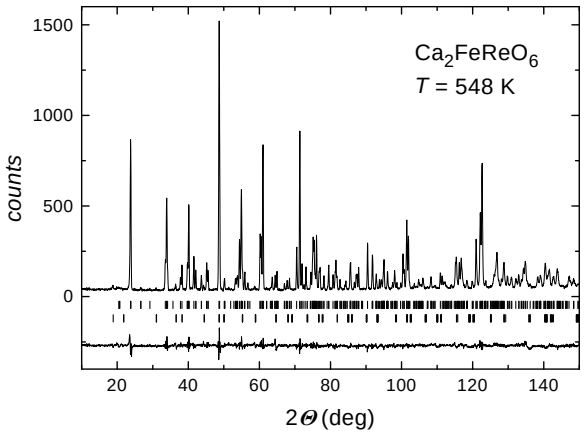

FIG. 1. Observed neutron diffraction pattern for CFRO at $T = 548$ K above T_C. The difference pattern arises from a refinement including the monolinic CFRO phase and the magnetite impurity phase (0.5%).

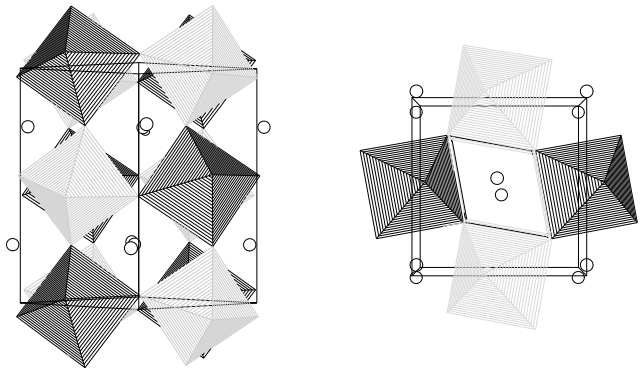

FIG. 2. a) View of the unit cell along the crystallographic (110) direction corresponding to a pseudocubic a or b axis. The monoclinic rock-salt arrangement of the Fe (black) and Re (grey) ions with opposite rotations of the octahedra along viewing direction can be seen.
b) View along the crystallographic (001) direction showing in phase rotations.

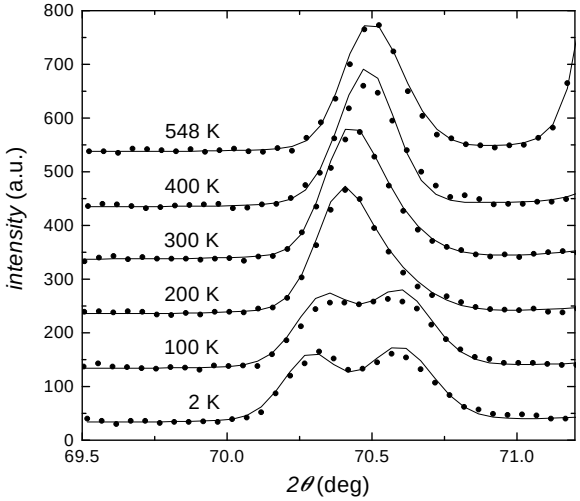

FIG. 3. Temperature dependence of the (040) reflection peak of CFRO. With decreasing temperature this peak with a large momentum transfer along the unique b axis broadens and finally splits into two reflections. Lines are from refinements including two crystallographic phases as described in the text.

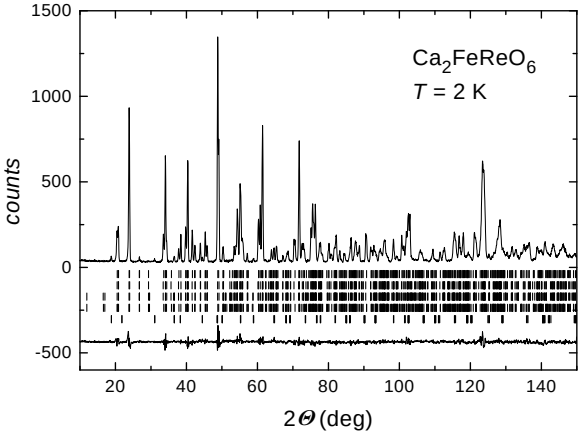

FIG. 4. Observed neutron diffraction pattern for CFRO at $T = 2$ K. The difference pattern arises from a refinement including the two magnetic monolinic CFRO phases and the magnetite impurity phase (0.5%).

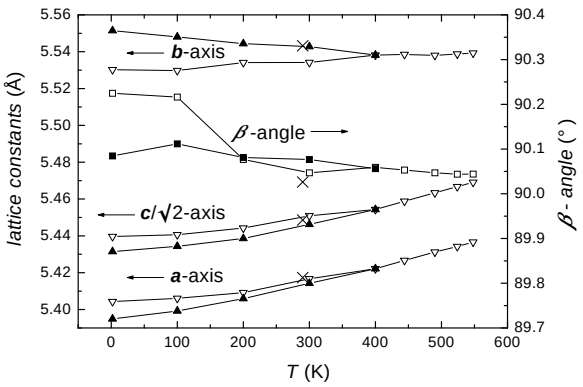

FIG. 5. Temperature dependence of the lattice constants (triangles) and the β-angle (squares) of the two different CFRO phases measured by neutron diffraction. The two phases merge to a single phase above room temperature. The results from X-ray diffraction (only one phase refined) at 290 K are shown by crosses.

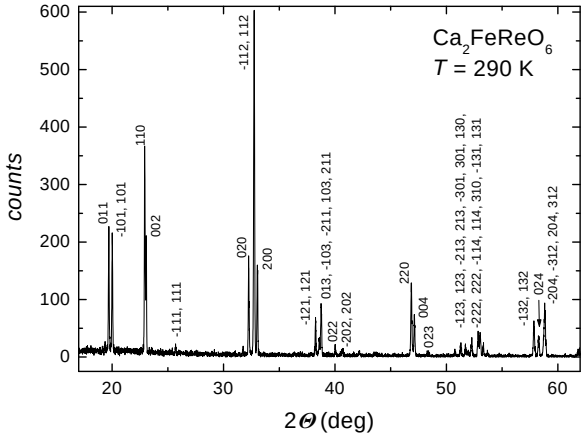

FIG. 6. X-ray powder diffraction pattern for CFRO taken at room temperature. The Bragg peaks are indexed in a monoclinic unit cell $a = 5.417(2)$ Å, $b = 5.543(2)$ Å, $c = 7.706(2)$ Å, and $\beta = 90.03(3)^\circ$ (space group $P2_1/n$).

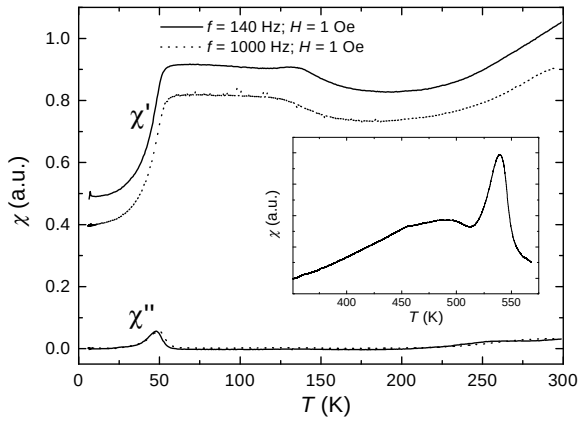

FIG. 7. Temperature dependence of the AC susceptibility of CFRO from 4 K up to 300 K. The inset shows the AC susceptibility above room temperature. Clearly a peak at the Curie temperature of 540 K can be seen.

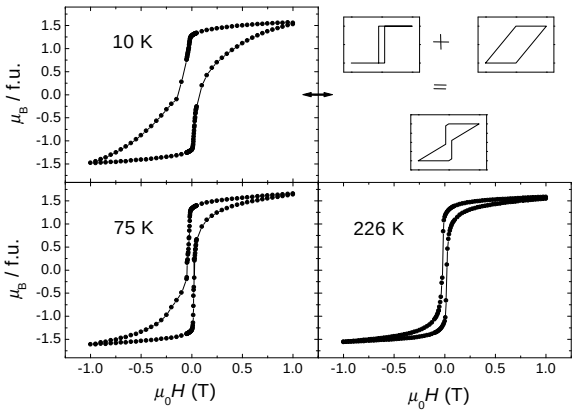

FIG. 8. Hysteresis loops of CFRO at constant temperatures of 10 K, 75 K, and 226 K, measured in magnetic fields from -1 T to 1 T. The unusual shape of the low temperature hysteresis curve results from two magnetic phases with high and low coercivity, as sketched in the figure.

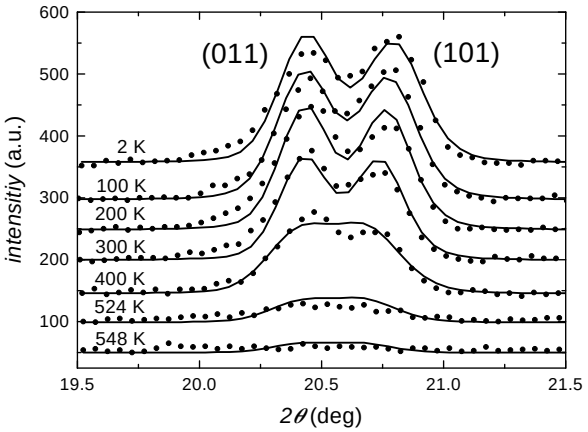

FIG. 9. Temperature dependence of the (011) and (101) Bragg peaks which are only visible in the ferromagnetic regime due to their magnetic origin.

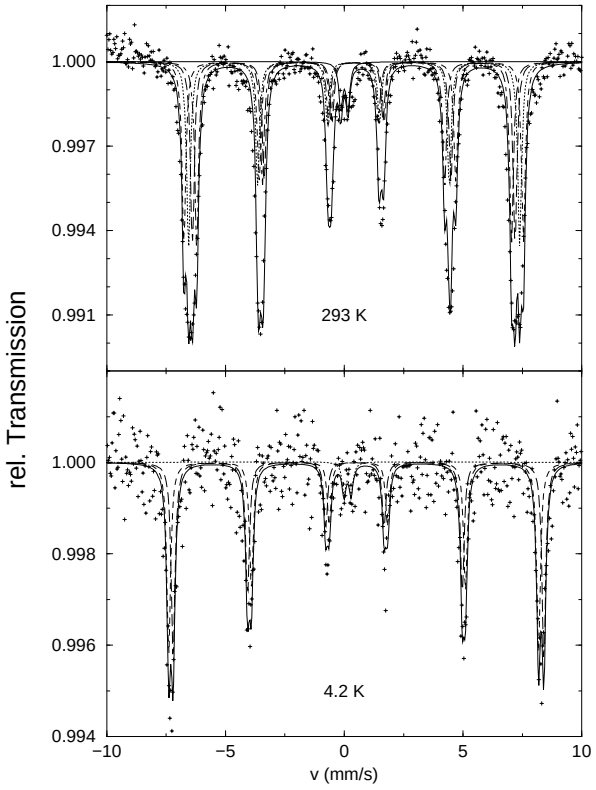

FIG. 10. ^{57}Fe-Mössbauer spectra of CFRO recorded at 4.2 K and 293 K. The total fit curve (solid line) is composed of a super-positioning of the lines for phase 1 (dotted and dotted-dashed) and for phase 2 (dashed and long dashed).

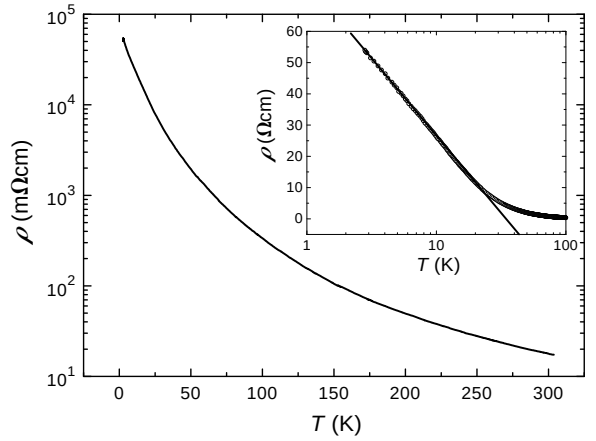

FIG. 11. Temperature dependence of the longitudinal resistivity. Above 110 K the resistivity is described by a variable range hopping like model. Below 20 K the resisitivity increases logarithmic with falling temperature as can be seen in the inset.

TABLE I. Positional and thermal paramaters of CFRO (space group $P2_1/n$) at 548 K. The R-factor was 4.4%.

Atom	Site	x	y	z	B (Å^2)
Ca	4e	0.0128(7)	0.0432(7)	0.7484(7)	1.11(8)
Fe	2d	$\frac{1}{2}$	0	0	0.63(5)
Re	2c	0	$\frac{1}{2}$	0	0.15(3)
O1	4e	0.2914(7)	0.2940(7)	0.9591(7)	0.69(7)
O2	4e	0.2996(7)	0.2918(7)	0.5389(7)	1.22(8)
O3	4e	0.9206(7)	0.4791(7)	0.7514(7)	0.94(7)

TABLE II. Positional and thermal paramaters of CFRO (space group $P2_1/n$) at 2 K. The R-factors for the two phases were 4.1% and 3.6%, respectively.

Phase	Atom	Site	x	y	z	B (Å^2)
	Ca	4e	0.0078(5)	0.0482(5)	0.7485(5)	0.14(5)
	Fe	2d	$\frac{1}{2}$	0	0	0.05(3)
1	Re	2c	0	$\frac{1}{2}$	0	0.00(1)
	O1	4e	0.2931(5)	0.2928(5)	0.9564(4)	0.45(4)
	O2	4e	0.3025(5)	0.2951(5)	0.5414(4)	0.37(4)
	O3	4e	0.9148(5)	0.4748(5)	0.7516(4)	0.35(4)
	Ca	4e	0.0158(5)	0.0503(5)	0.7517(4)	0.22(5)
	Fe	2d	$\frac{1}{2}$	0	0	0.06(3)
2	Re	2c	0	$\frac{1}{2}$	0	0.00(1)
	O1	4e	0.2990(5)	0.2993(5)	0.9531(4)	0.33(4)
	O2	4e	0.2944(5)	0.2917(5)	0.5439(4)	0.38(4)
	O3	4e	0.9171(5)	0.4749(5)	0.7516(4)	0.35(4)

TABLE III. Lattice constants and β angles as a function of temperature of the two phases. Above 300 K the two phases merge to a single phase.

	Phase 1				Phase 2			
T (K)	a (Å)	b (Å)	c (Å)	β (deg)	a (Å)	b (Å)	c (Å)	β (deg)
2	5.4043(5)	5.5303(7)	7.6923(5)	90.225(4)	5.3949(5)	5.5515(7)	7.6812(5)	90.085(4)
100	5.4060(5)	5.5297(7)	7.6942(5)	90.216(4)	5.3992(5)	5.5480(7)	7.6853(5)	90.112(4)

200	5.4091(5)	5.5341(7)	7.6997(5)	90.077(4)	5.4059(5)	5.5444(7)	7.6913(5)	90.081(4)
300	5.4167(5)	5.5342(7)	7.7091(5)	90.047(4)	5.4142(5)	5.5428(7)	7.7021(5)	90.077(4)
400	5.4222(5)	5.5382(5)	7.7136(5)	90.059(4)	-	-	-	-
444	5.4267(5)	5.5385(5)	7.7199(5)	90.053(4)	-	-	-	-
490	5.4312(5)	5.5380(5)	7.7264(5)	90.047(4)	-	-	-	-
524	5.4342(5)	5.5387(5)	7.7311(5)	90.044(4)	-	-	-	-
548	5.4366(5)	5.5393(5)	7.7344(5)	90.044(4)	-	-	-	-

TABLE IV. Bond lengths and bond angles for CFRO at 2 K and 548 K.

Temperature	2 K		548 K
Phase	**1**	**2**	
Main bond lengths of FeO_6 octahedra (Å)			
Fe—O1	1.9955	2.0163	2.0094
Fe—O2	2.0134	1.9930	2.0181
Fe—O3	1.9960	1.9892	1.9954
Main bond lengths of ReO_6 octahedra (Å)			
Re—O1	1.9846	1.9937	1.9781
Re—O2	1.9765	1.9918	1.9725
Re—O3	1.9686	1.9640	1.9737
Bond angles (deg)			
Fe—O1—Re (×2)	152.524	149.691	153.423
Fe—O2—Re (×2)	151.383	152.490	153.046
Fe—O3—Re (×2)	151.909	152.581	153.970
Short bond lengths Ca—O (Å)			
Ca—O1	2.3770	2.3279	2.3700
Ca—O1	2.5972	2.5751	2.6222
Ca—O1	2.6735	2.7052	2.6953
Ca—O2	2.3684	2.3600	2.3840
Ca—O2	2.6379	2.5710	2.6376
Ca—O2	2.6604	2.6910	2.6891
Ca—O3	2.3196	2.3728	2.3828
Ca—O3	2.4123	2.4166	2.4662

TABLE V. Mössbauer parameters, δ: isomer shift, $B_{\rm hf}$: hyperfine field, and $\Delta E_{\rm Q}$: quadrupole splitting.

T (K)	Iron Site	δ (mm/s)	$B_{\rm hf}$ (T)	$\Delta E_{\rm Q}$ (mm/s)	Ratio
293	1 a	0.477(6)[a]	44.32(5)	−0.16(1)[a]	0.494(5)[a]
	1 b	0.477(6)	42.11(5)	−0.16(1)	0.494(5)
	2 a	0.401(5)[b]	43.22(5)	+0.03(1)[b]	0.506(5)[b]
	2 b	0.401(5)	41.10(5)	+0.03(1)	0.506(5)
4.2	1	0.495(7)	48.27(4)	−0.20(1)	0.494(5)[c]
	2	0.524(6)	48.39(4)	+0.15(1)	0.506(5)[c]

[a]correlated with iron site 1 b, [b]correlated with iron site 2 b, [c]ratio taken from ambient temperature spectrum